A β-Amyloid$_{(1-42)}$ Biosensor Based on Molecularly Imprinted Poly-Pyrrole for Early Diagnosis of Alzheimer's Disease

Rezvan Dehdari Vais[1], Hossein Yadegari[2], Hossein Heli[3]*, Naghmeh Sattarahmady[3,4]

[1]PhD Candidate, Nanomedicine and Nanobiology Research Center, Shiraz University of Medical Sciences, Shiraz, Iran
[2]PhD, Department of Mechanical and Materials Engineering, University of Western Ontario, London, Ontario N6A 5B9, Canada
[3]PhD, Nanomedicine and Nanobiology Research Center, Shiraz University of Medical Sciences, Shiraz, Iran
[4]PhD, Department of Medical Physics, School of Medicine, Shiraz University of Medical Sciences, Shiraz, Iran

ABSTRACT

Background: Alzheimer's disease (AD) is a common form of dementia, characterized by production and deposition of β-amyloid peptide in the brain. Thus, β-amyloid peptide is a potentially promising biomarker used to diagnose and monitor the progression of AD.

Objective: The study aims to develop a biosensor based on a molecularly imprinted poly-pyrrole for detection of β-amyloid.

Material and Methods: In this experimental study, an imprinted poly-pyrrole was employed as an artificial receptor synthesized by electro-polymerization of pyrrole on screen-printed carbon electrodes in the presence of β-amyloid. β-amyloid acts as a molecular template within the polymer. The biosensor was evaluated by cyclic voltammetry using ferro/ferricyanide marker. The parameters influencing the biosensor performance, including electro-polymerization cycle umbers and β-amyloid binding time were optimized to achieve the best biosensor sensitivity.

Results: The β-amyloid binding affinity with the biosensor surface was evaluated by the Freundlich isotherm, and Freundlich constant and exponent were obtained as 0.22 ng mL^{-1} and 10.60, respectively. The biosensor demonstrated a detection limit of 1.2 pg mL^{-1}. The biosensor was applied for β-amyloid determination in artificial cerebrospinal fluid.

Conclusion: The biosensor is applicable for early Alzheimer's disease detection.

Citation: Dehdari Vais R, Yadegari H, Heli H, Sattarahmady N. A β-Amyloid$_{(1-42)}$ Biosensor Based on Molecularly Imprinted Poly-Pyrrole for Early Diagnosis of Alzheimer's Disease. *J Biomed Phys Eng.* 2021;11(2):215-228. doi: 10.31661/jbpe.v0i0.1070.

Keywords

Beta-Amyloid; β-Amyloid (1-40); Molecular Imprinting; Artificial Antibody; Neurodegenerative Disease; Sensory Aids; Biosensing Technique; Bioprobe

Introduction

Alzheimer's disease (AD) is a neurodegenerative disorder characterized by memory loss and cognitive dysfunction; it is a common form of dementia. It is investigated that about 80 million people will be afflicted with AD in 2050 [1]. AD is caused due to the production and deposition in the brain of β-amyloid peptides that included 39 to 42 amino acid residues [2]. Although positron emission tomography imaging shows cortical amyloid pathology with cognitive criteria [3, 4], early diagnosis of AD stage has still been of great significance.

Disease biomarkers are detectable indicators of the disease states,

*Corresponding author:
Hossein Heli
Nanomedicine and Nanobiology Research Center, Shiraz University of Medical Sciences, Shiraz, Iran
E-mail: hheli7@yahoo.com

Received: 9 December 2018
Accepted: 23 January 2019

which can be specific molecules, genes, antigens, proteins, cells, or hormones. Detection of biomarkers is the new route of the disease state and its diagnosis. Along this line, different categories of biosensors have been introduced for the biomarker detection, including aptasensors [5], genosensors [6, 7], non-enzymatic biosensors [8, 9], and immunosensors [10]. For fabrication of the biosensors, nanomaterials with special size and shape have been applied as transducers [11-13]. Among these nanobiosensors, electrochemical transduction is sensitive, simple, robust, low-cost, and miniaturizable, and works with small sized samples [13]. Nanomaterials, as components of the electrochemical nanobiosensors (transducer or else), make them more sensitive and selective due to the unique redox properties, chemical stability and tuneability of covering the substrates [5, 6, 8, 9, 11-14].

As an indicator of AD, β-amyloid peptides, and specially β-amyloid$_{(1-42)}$, are promising biomarkers used to diagnose and monitor the progression of AD [15]. Up to now, the techniques of ELISA [16], different modes of mass spectrometry (MS) [17-22], immunosensors [23], scanning tunneling electron microscopy [24], magnetic resonance imaging [25], fluorimetry [26], in vivo optical imaging [27, 28], positron emission tomography [29, 30] and surface plasmon resonance [31] have been reported for detection of β-amyloid for AD diagnosis. However, the ELISA method suffers from high limits of quantitation, high costs of enzyme-linked antibodies and consumption time. On the other hand, new modes of MS, including time-of-flight secondary ion MS [17], on-line immunoaffinity-liquid chromatography-MS [18], hydrogen exchange with top-down electron capture dissociation MS [19], matrix-assisted laser desorption ionization-time-of-flight MS [20], column-switching liquid chromatography-tandem MS [21], and covalent chiral derivatized ultraperformance liquid chromatography-tandem MS [22] have the disadvantages of relative insensitivity, complexicity, high cost, time-consuming and difficulty for β-amyloid determination. The immunosensors have disadvantages arising from the instability of antibodies. Therefore, there is a need to fabricate novel sensing devices for β-amyloid determination.

Molecular imprinting technology is a tailor-made recognition capability for (template) molecules at the molecular level using molecularly imprinted polymers (MIPs). The template molecule can be memorized with a high affinity with specific binding sites in the cross-linked polymer matrix. Subsequent removal of the template reveals binding sites that are complementary in size and shape to the original imprinted template molecule [32]. Upon rebinding, MIPs recognize the template molecule with a high selectivity. In MIPs, a retention mechanism based on molecular recognition is dominated like immunosorbents. As a result, MIPs are often named as synthetic antibodies, while they offer better handling, stability (toward acids, bases, ions and organic solvents), lower costs, high pressure resistance, wide working temperature range and ease of preparation [32], compared to antibody-based routes making them attractive for numerous applications. MIPs have been successfully applied as an alternative tool over the biological entities in several medicinal fields such as drug delivery, cell recognition, and protein recognition [33-35].

Until now, MIPs-based biosensors have been developed for the detection of biomarkers such as troponin I [36], troponin T [37], prostate-specific antigen [38], myoglobin [39], microRNA [40] and neopterin [41]. However, β-amyloid detection using MIPs has not been approached. In the present study, a MIP-based biosensor for determination of β-amyloid was prepared to apply for early detection of AD.

Material and Methods

In this experimental study, all chemicals used throughout this study were of analytical grade from Scharlau (Spain) or Merck (Germany)

and employed without further purification. Double distilled water was used to prepare all aqueous solutions. Lyophilized β-amyloid$_{(1-42)}$ peptide was purchased from Sigma (USA). Deionized water was used for solutions preparation.

Electrochemical experiments were carried out using a μ-Autolab potentiostat/galvanostat (the Netherlands) interfaced to a PC with GPES 4.9 software. Screen printed carbon electrodes (SPCEs) were purchased from DropSens (Spain) and employed for all measurements.

In the optimized preparation conditions of the biosensor, an electrochemical pretreatment of SPCEs was firstly done in 100 mmol L^{-1} Tris-HCl buffer, pH= 7.4 (Tris) at 1.2 V for 60 s, followed by rinsing the electrode surface with Tris. Afterward, 30 μL of the polymerization solution containing 100 mmol L^{-1} pyrrole monomer and 1.29 μg mL^{-1} β-amyloid$_{(1-42)}$ (as a template) prepared in Tris was placed on the pretreated SPCE surface. Electro-polymerization was then carried out by cyclic voltammetry (CV) in a potential range between -0.1 to 0.8 V with a potential sweep rate of 50 mV s^{-1} for five consecutive cycles. After electro-polymerization process, the removal of template molecule from the polymeric layer was performed by immersing the electrode into 5.0 mmol L^{-1} aqueous solution of oxalic acid at room temperature for 24 h. The resultant MIP film was then washed with Tris and applied as the working electrode for all electrochemical measurements described below. A NIPE was prepared under the same experimental conditions without the presence of β-amyloid$_{(1-42)}$ template in the electro-polymerization solution. The stepwise fabrication process of the biosensors is schematically presented in Figure 1.

CV was employed to investigate the analytical performance of the biosensor at different concentrations of β-amyloid$_{(1-42)}$ in Tris and artificial cerebrospinal fluid (CSF). Initially, the biosensor was incubated in solutions of β-amyloid$_{(1-42)}$ at 37 °C for 20 min. After that, the biosensor was washed with Tris to remove non-bonded β-amyloid$_{(1-42)}$, and the CV measurements were carried out from -0.35 to 0.35 V with a potential sweep rate of 50 mV s^{-1} in 0.5 mmol L^{-1} $K_3[Fe(CN)_6]/K_4[Fe(CN)_6]$ 1:1

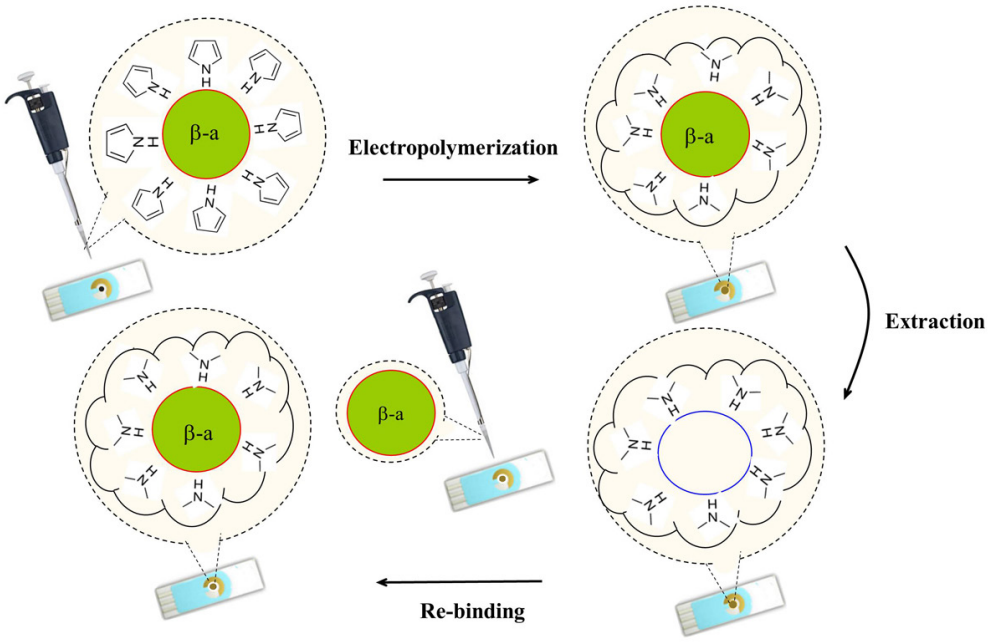

Figure 1: The stepwise fabrication process of the biosensors.

mixture prepared in Tris.

An artificial CSF was made with a composition of NaCl 126 + NaH_2PO_4 1.24 + $NaHCO_3$ 26 + KCl 2.5 + $MgSO_4$ 1.2 + $CaCl_2$ 2.0 + D-glucose 10 mmol L^{-1}, pH=7.35, and with a stream of 95% air + 5% CO_2 was saturated. β-amyloid$_{(1-42)}$ of different concentrations were prepared in the artificial CSF, diluted with Tris of the final dilution ratio of 1:1, and found by the biosensor.

Results

Electro-polymerization of pyrrole was performed in the synthesis solution containing β-amyloid$_{(1-42)}$ as a molecular template, as described in section 2.3. β-amyloid$_{(1-42)}$ binding into the active sites of the biosensor surface was electrochemically monitored through repression of the redox kinetic of the $K_3[Fe(CN)_6]/K_4[Fe(CN)_6]$ marker. To optimize the working conditions of the biosensor, anodic peak currents in cyclic voltammograms of the biosensor were measured upon re-binding by β-amyloid$_{(1-42)}$ of 3.0 ng mL^{-1}.

Because the thickness of PPy film has a significant influence on the biosensing of β-amyloid$_{(1-42)}$, it was changed by alterations in the potential cycle number during the electro-polymerization. For this purpose, PPy was synthesized using different potential cycles, and evaluated before and after capturing β-amyloid$_{(1-42)}$ of 3.0 ng mL^{-1}; the results are presented in Figure 2A. To judge about the best potential cycle number for the synthesis of PPy, the anodic peak currents were measured and their differences before and after capturing the target are plotted versus cycle number in Figure 2B. Selection of the anodic peak was due to the more sharpness of this peak, compared to the cathodic counterpart. Based on the results, the highest peak currents, and more importantly, the highest peak current difference before and after β-amyloid$_{(1-42)}$ capturing was attained for PPy synthesis with five potential cycles. These results indicated that up to five cycles, the MIP layer

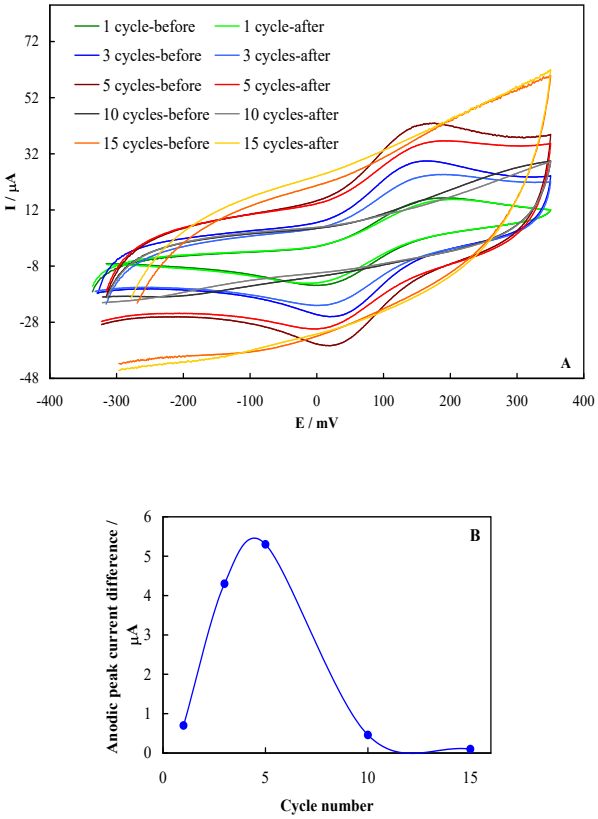

Figure 2: (A) Cyclic voltammograms recorded before and after binding of the biosensor with β-amyloid$_{(1-42)}$ for different potential cycles of 1, 3, 5, 10 and 15. (B) Dependency of the anodic peak current difference (difference of before β-amyloid$_{(1-42)}$ binding and after that) on the cycle numbers of the molecularly imprinted polymer (MIP) synthesis.

thickened leading to better formation of the β-amyloid$_{(1-42)}$-resembled holes in the bulk of the polymer. However, more cycles of potential lead to formation of a very thick polymeric layer and inhibition of the marker accessibility to the underlying current collector (vie infra, Figure 3). Therefore, the best sensitivity was attained with five potential cycles of PPy synthesis, and also employed for further studies.

Another parameter that should be optimized for a MIP-base biosensor is the biosensor surface-target binding time. The biosensor was incubated with β-amyloid$_{(1-42)}$ of 3.0 ng

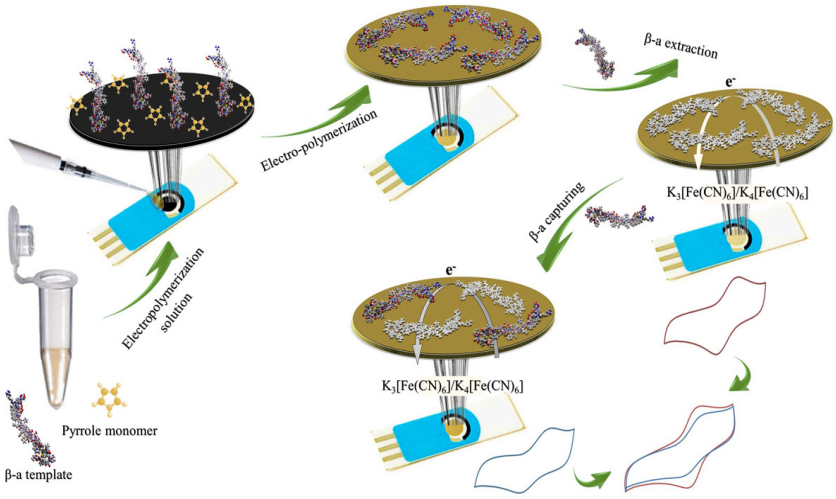

Figure 3: The fabrication processes and signal generation of the biosensor.

mL^{-1} at room temperature for different binding times of 3, 5, 10, 20, 30 and 40 min; cyclic voltammograms were recorded, as shown in Figure 4. According to these results, the peak current decrement continued upon time prolonging up to 20 min and then remained almost constant. Therefore, a binding time of 20 min was selected for β-amyloid$_{(1-42)}$) targeting.

For the elution of the bond β-amyloid$_{(1-42)}$ from the biosensor surface after fabrication of a new biosensor or after already binding for reusing, alkaline and organic compounds-containing solvents were not suitable because the screen-printed electrodes were pulled up in these solutions. Our results also showed that mineral acids and acetic acid/surfactant mixtures could not elute β-amyloid$_{(1-42)}$ from the biosensor, while a 5.0 mmol L^{-1} oxalic acid solution at room temperature overnight successfully eluted the target, and this later eluent was employed thereafter.

In order to quantitate the β-amyloid$_{(1-42)}$ by the biosensor, cyclic voltammograms were recorded after binding with different concentrations of β-amyloid$_{(1-42)}$, and are shown in Figure 5A. Upon increment in the β-amyloid$_{(1-42)}$ concentration, the peak current was lowered due to blockage of the pinholes at the MIP surface by the target and prevention of ac-

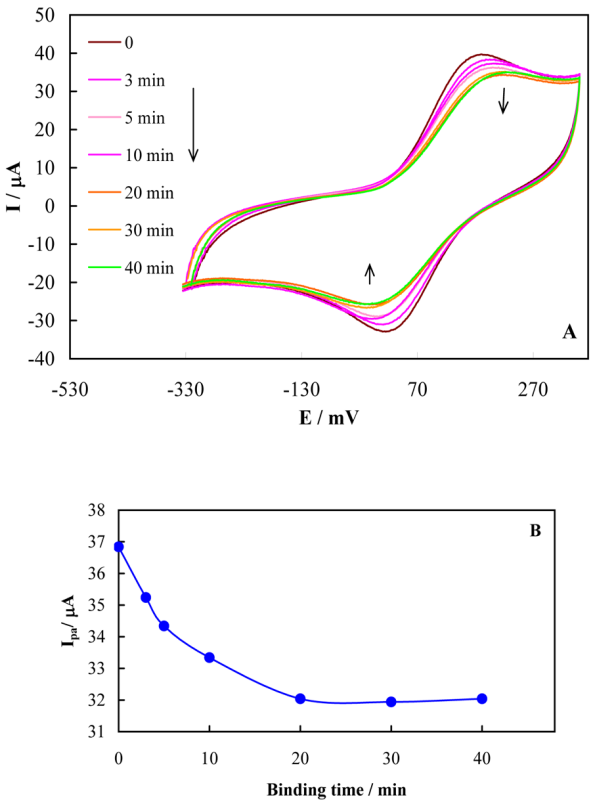

Figure 4: (A) Cyclic voltammograms recorded using the biosensor before and after capturing β-amyloid$_{(1-42)}$ at different binding times of 3, 5, 10, 20, 30 and 40 min. (B) Dependency of the anodic peak current on the binding time of β-amyloid$_{(1-42)}$.

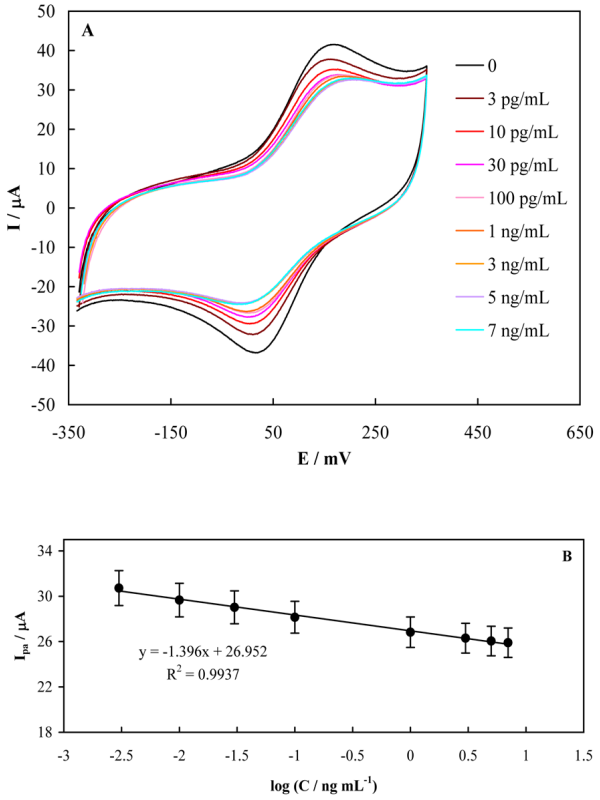

Figure 5: (A) Cyclic voltammograms recorded using the biosensor before and after capturing different concentrations of β-amyloid$_{(1-42)}$. (B) The dependency of the peak currents on the β-amyloid$_{(1-42)}$ concentration (calibration curve).

cessibility of the redox marker for electron exchange. At the higher concentrations, therefore, a surface saturation happened, and the rate of the current decrement was slow. Despite the fact that PPy is a conducting polymer, it has a limited conductivity in Tris-buffer of 100 mmol L^{-1}, pH=7.4 (working conditions of the biosensor) and represses the kinetics of charge transfer of the redox marker. Thus, a limited current is passed, which is important and appropriate when NIPE is evaluated (see below). On the other side, the subsequent elution of the β-amyloid$_{(1-42)}$ template during the biosensor preparation formed lots of pores with a protein-resembled shape. This porous structure supplies a network for the marker to attain the underneath carbon substrate, and a signal for the marker is recordable. Capturing β-amyloid$_{(1-42)}$ by the biosensor blocks the holes and limits the redox marker accessibility to the carbon substrate for electron transfer. Therefore, the current depends on the β-amyloid$_{(1-42)}$ blocking level of the biosensor. The fabrication processes and signal generation of the biosensor are schematically depicted in Figure 3.

On the basis of the data presented in Figure 5A, the dependency of the peak currents on the β-amyloid$_{(1-42)}$ concentration can be derived, as shown in Figure 5B. The peak current dependency was linear in a concentration range of 0.003-7 ng mL^{-1}, and the trend line had a regression equation of y = -(1.39 ± 0.045)x + (26.96 ± 0.062). The use of the standard deviation of the anodic peak current in the absence of the target (the blank signal), and the slope of the calibration curve are presented in Figure 5B, the limit of detection (LOD) of β-amyloid$_{(1-42)}$ by the biosensor was calculated.

In order to evaluate the importance of the surface imprinting on biosensor function, we fabricated a NIPE, and recorded the cyclic voltammograms in the presence of different concentrations of β-amyloid$_{(1-42)}$, as depicted in Figure 6. The data indicated that NIPE did not generate significant signals upon varying the β-amyloid$_{(1-42)}$ concentration.

An isotherm for estimation of β-amyloid$_{(1-42)}$ binding affinity into the biosensor at different concentrations can be plotted, using the data presented in Figure 5A. The models of Langmuir [42], Freundlich [43] and two-type simultaneous binging [44] were examined. The best fitting for the peak current-β-amyloid$_{(1-42)}$ concentration was attained based on the Freundlich adsorption isotherm, using the following equation:

$$(I_{pa0} - I_p) / I_{pa0} = K \times C^{1/n} \qquad (1)$$

where $(I_{pa0} - I_p) / I_{p0}$ indicates that the amount of β-amyloid$_{(1-42)}$ captured at a concentration of C, and I_{pa0} is the anodic peak current in the absence of β-amyloid$_{(1-42)}$; I_p is the anodic peak

current in the presence of β-amyloid$_{(1-42)}$. In addition, K is the Freundlich constant, and n is the Freundlich exponent. Figure 7 shows the corresponding isotherm based on the Freundlich adsorption isotherm for the biosensor. The results indicated that the amount of the captured β-amyloid$_{(1-42)}$ gradually decreased upon increment in the β-amyloid$_{(1-42)}$ concentration, and then reached an adsorption plateau at 5 ng mL^{-1}. The adsorption plateau is the re-

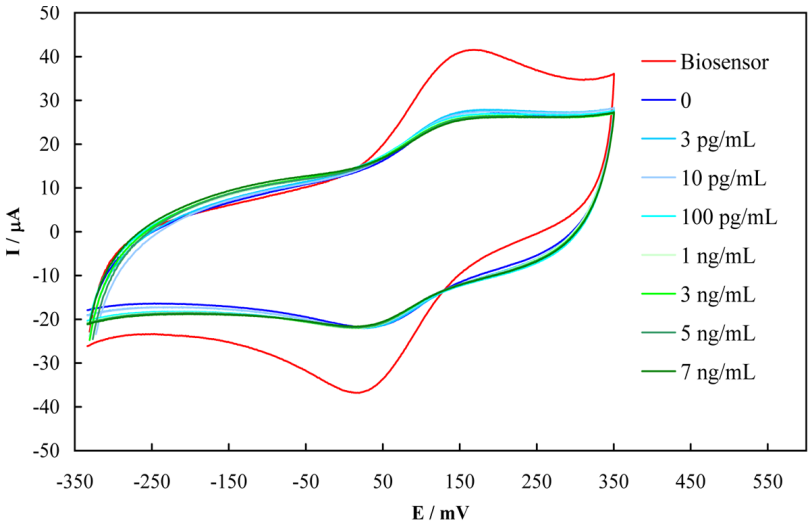

Figure 6: Cyclic voltammogram recorded using the biosensor (voltammogram with the highest peak currents), and cyclic voltammograms recorded using Non-molecularly imprinted polymer electrode (NIPE) before and after capturing different concentrations of β-amyloid$_{(1-42)}$.

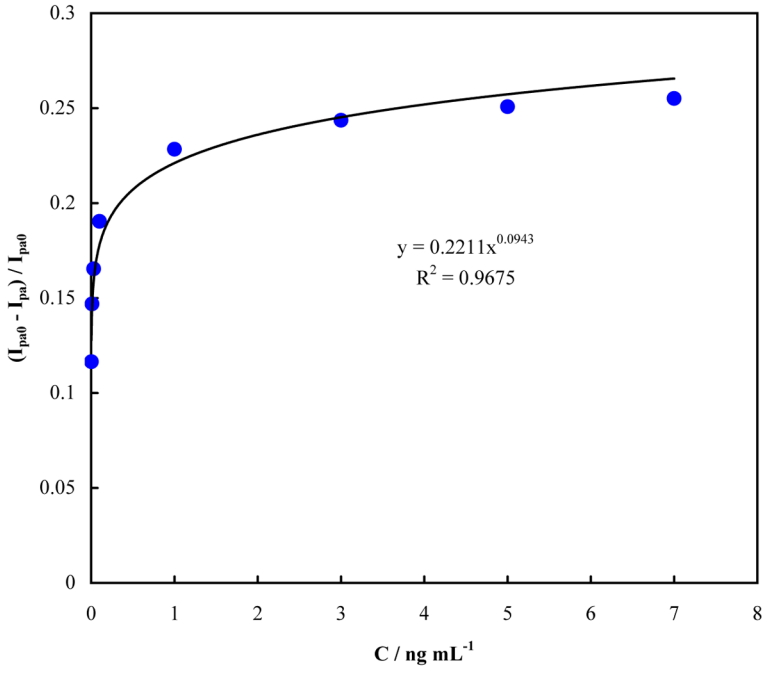

Figure 7: Dependency of (I_{pa0} - I_p) / I_{pa0} on the concentration of β-amyloid$_{(1-42)}$ and the fitting curve based on the Freundlich adsorption isotherm.

sult of saturation of binding sites at the biosensor surface by β-amyloid$_{(1-42)}$. Using the regression equation in Figure 7, we obtained K and n values as 0.22 ng mL^{-1} and 10.60, respectively. The high value obtained for n confirmed that the amount of the bound β-amyloid$_{(1-42)}$ greatly increased with a small change in the concentration (at its low concentrations), while more imprinted sites were rebounded, and the adsorption intensity weakened and eventually remained constant (at its high concentrations); later, saturation occurred and the current ratio remained constant.

For evaluation of the biosensor capability for β-amyloid$_{(1-42)}$ detection in real samples, β-amyloid$_{(1-42)}$ of different concentrations was supplemented into CSF and cyclic voltammograms were recorded, as shown in Figure 8A. Upon increment in the β-amyloid$_{(1-42)}$ concentration, the peak current was lowered similarly as observed for the β-amyloid$_{(1-42)}$quantitation in Tris. A calibration curve was also plotted for the data, which shown in Figure 8B. Based on this calibration curve, β-amyloid$_{(1-42)}$ could be determined in CSF by a sensitivity of 1.09 μA mL ng^{-1} and a LOD of 2.3 pg mL^{-1}.

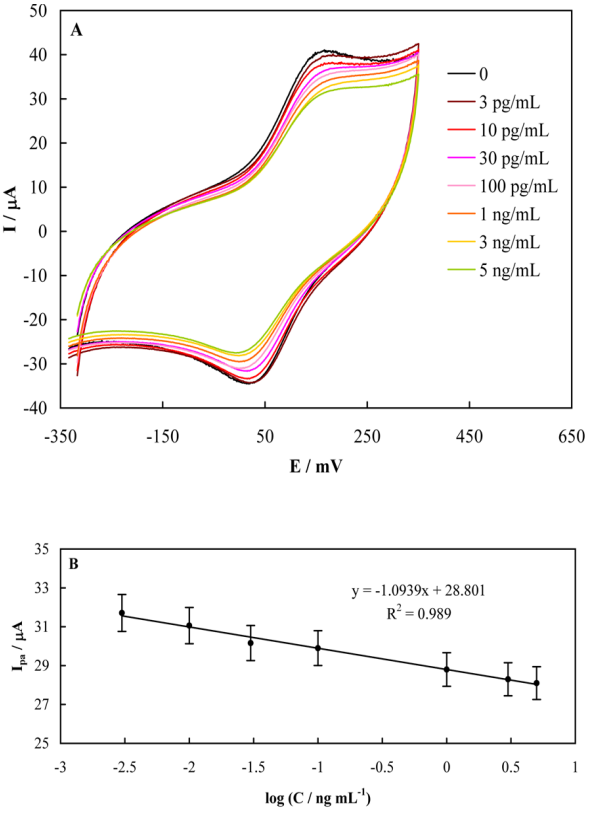

Figure 8: A) Cyclic voltammograms recorded using the biosensor before and after capturing different concentrations of β-amyloid$_{(1-42)}$ in artificial cerebrospinal fluid (CSF). (B) The dependency of the peak currents on the β-amyloid$_{(1-42)}$ concentration (calibration curve).

Discussion

MIPs-based biosensors, as artificial receptors, provide an alternative method for selective recognition of biomolecules. The process of molecular imprinting includes the creation of a polymeric film with selective recognition cavities based on a biomolecular template [32]. In the present study, poly-pyrrole (PPy) polymer which synthesized in the presence of β-amyloid$_{(1-42)}$ template, was employed to fabricate the biosensor because it can be formed electrochemically and stably at neutral (physiological) pHs that are important for the biosensor applications in biological sample analyses [45]. For removing of template from the biosensor surface, it should be mentioned that different solvents might be employed. A literature review on the solvents employed for protein elution from MIPs is summarized in Table 1. The reported solvents include mineral acids and bases, and organic solutes or solvents dissolved in aqueous solutions, accompanied with or without employment of a surfactant. In this research, the oxalic acid solution can successfully eluted β-amyloid$_{(1-42)}$ template. The designed biosensor could successfully detect β-amyloid$_{(1-42)}$ with a LOD of as 1.2 pg mL^{-1} which is comparable with different methods of amyloid detection (Table 2). In order to evaluate the actual performance of biosensor, it was applied for β-amyloid$_{(1-42)}$ determination in artificial CSF with high sensitivity and selectivity, confirming the biosensor applicability for AD diagnosis.

Table 1: Different solvents reported for protein elution from molecularly imprinted polymers (MIPs).

Protein	Eluent	Reference
Avidin	Chloroform	[46]
Ferritin	5 mmol L^{-1} NaOH	[47]
Troponin T	Ethanol:water (2:1 V/V) + 0.25 mol L^{-1} NaOH	[48]
Myoglobin	Proteinase K	[49]
Cytochrome C	1 mol L^{-1} H_2SO_4	[50]
Immunoglobulin G	3 mol L^{-1} NaCl + 0.1% sodium dodecyl sulfate	[51]
Bovine hemoglobin	1 mol L^{-1} oxalic acid	[52]
Bovine hemoglobin	10% Acetic acid + 10% sodium dodecyl sulfate	[53]
Acetylcholinesterase	Glycine-HCl	[54]
Bovine serum albumin	5% Acetic acid + 10% sodium dodecyl sulfate	[55]
Bovine serum albumin	5% Acetic acid + 10% sodium dodecyl sulfate	[56]
Human serum albumin	30% NaOH	[57]
Ovarian cancer antigen	1% Acetic acid + 3% sodium dodecyl sulfate	[58]
Bovine leukemia virus glycoproteins	1 mol L^{-1} H_2SO_4	[59]

Conclusion

A synthetic β-amyloid$_{(1-42)}$ receptor was designed using molecular imprinting approach to fabricate a biosensor. The biosensor represented a high affinity and sensitivity. The receptor was fabricated by electro-polymerization of pyrrole on carbon screen-printed electrodes in the presence of β-amyloid$_{(1-42)}$ as a template. Formation of a thin MIP layer was critical to improve the signals as well as the performance of the biosensor towards the target β-amyloid$_{(1-42)}$. The resultant β-amyloid$_{(1-42)}$ receptor was examined by recording electrochemical signals of the ferro/ferricyanide redox probe after the β-amyloid$_{(1-42)}$ binding process. At the same time, successful elution of β-amyloid$_{(1-42)}$ was achieved from the MIP surface. A Freundlich isotherm fitting revealed a high affinity of the receptor toward the imprinted β-amyloid$_{(1-42)}$. β-amyloid$_{(1-42)}$ binding onto the biosensor imposed a significant decrement in the peak current of the redox marker and provided a calibration curve with a linear dependency of the peak currents on the β-amyloid$_{(1-42)}$ concentration. A very low LOD value was attained, compared to other reported techniques, confirming the applicability of the biosensor for β-amyloid$_{(1-42)}$ detection at a clinically relevant level.

Acknowledgment

This research was a part of R. Dehdari Vais's PhD thesis (21735). The financial support of the Iran National Science Foundation Grant NO. 96005985 is gratefully acknowledged. We would also like to thank the Research Councils of Shiraz University of Medical Sciences.

Conflict of Interest

None

References

1. Brookmeyer R, Johnson E, Ziegler-Graham K, Arrighi HM. Forecasting the global burden of Alzheimer's disease. *Alzheimer's & Dementia.* 2007;**3**(3):186-91. doi: 10.1016/j.jalz.2007.04.381. PubMed PMID: 19595937.
2. Murphy MP, LeVine III H. Alzheimer's disease and the amyloid-β peptide. *J Alzheimers Dis.* 2010;**19**(1):311-23. doi: 10.3233/JAD-2010-1221. PubMed PMID: 20061647. PubMed PMCID:

Table 2: Comparison of different methods of amyloid detection.

Amyloid type	Method	Detecting element	Linear range	LOD	Reference
β-amyloid$_{(1-42)}$	Electrochemistry	Anti mAβ/protein G/ SAM/AuNPs	0.01-100 nmol L^{-1}	0.57 nmol L^{-1}	[60]
β-amyloid$_{(1-40)}$	Electrochemistry	Anti mAβ/pyrenyl groups	1-200 µmol L^{-1}	2.04 µmol L^{-1}	[60]
β-amyloid$_{(1-40)}$	Electrochemistry	Anti mAβ/SAM/ AuNPs	1-1000 nmol L^{-1}	2.65 nmol L^{-1}	[60]
β-amyloid$_{(1-40)}$	Electrochemistry	Antibody	0.01-100 nmol L^{-1}	10 pmol L^{-1}	[61]
β-amyloid$_{(1-40/1-42)}$	Electrochemistry	Antibody	0.2-40 nmol L^{-1}	50 pmol L^{-1}	[62]
β-amyloid$_{(1-42/1-16)}$	Electrochemistry	Antibody	0-0.5 nmol L^{-1}	5 pmol L^{-1}	[63]
β-amyloid$_{(1-40)}$	Fluorescence	Aptamer	0-70 nmol L^{-1}	3.57 nmol L^{-1}	[64]
β-Amyloid$_{(1-42)}$	Electrochemistry	Biotinylated PrP^{C} (95-110) peptide	10^{-6}-1 µmol L^{-1}	0.5 pmol L^{-1}	[65]
β-amyloid$_{(1-42)}$	Fluorescence	Antibody-magnetic nanoparticle	10-3000 pg mL^{-1}	20 pg mL^{-1}	[66]
β-amyloid$_{(1-40)}$	Fluorescence	Antibody-magnetic nanoparticle	10-4000 pg mL^{-1}	20 pg mL^{-1}	[66]
β-amyloid$_{(1-40)}$	SPR	Antibody	-	3.3 pmol L^{-1}	[67]
β-amyloid$_{(1-42)}$	SPR	Antibody	-	3.5 pmol L^{-1}	[67]
β-amyloid$_{(1-42)}$	Electrochemistry	Antibody/AuNPs	0.001-10 ng mL^{-1}	1 pg mL^{-1}	[68]
β-amyloid$_{(1-42)}$	ECL	Antibody	0.73-3000 pg mL^{-1}	1.24 pg mL^{-1}	[69]
β-amyloid$_{(1-40/1-42/1-16)}$	Electrochemistry	Heme β-amyloid$_{(1-16)}$-AuNPs/ mAb	0.02-1.50 nmol L^{-1}	10 pmol L^{-1}	[70]
β-amyloid$_{(1-42)}$	LSPR	Antibody	<10 pmol L^{-1}	<100 fmol L^{-1}	[71]
β-amyloid$_{(1-42)}$	LSPR	Single gold nanoparticle	10^{-6}-100 µmol L^{-1}	1.5 pmol L^{-1}	[72]
β-amyloid	Electrochemistry	Antibody-Aptamer	0.5-30 nmol L^{-1}	100 pmol L^{-1}	[73]
β-amyloid$_{(1-42)}$	Electrochemistry	Antibody-AuNPs	10-1000 pg mL^{-1}	5.2 pg mL^{-1}	[74]
β-amyloid$_{(1-42)}$	Electrochemistry	Antibody	0.5-500 ng mL^{-1}	0.1 ng mL^{-1}	[75]
β-amyloid$_{(1-42)}$	Electrochemistry	Antibody	-	-	[76]
β-amyloid$_{(1-42)}$	Bio-barcode detection	Antibody	0.1-100 fmol L^{-1}	100 amol L^{-1}	[77]
β-amyloid$_{(1-42)}$	Microarray	Matched antibody pair	0-5 ng mL^{-1}	73.07 pg mL^{-1}	[78]
β-Amyloid$_{(1-42)}$	Electrochemistry	Oligopeptide	0.48-12 nmol L^{-1}	240 pmol L^{-1}	[79]
β-amyloid$_{(1-42)}$	Electrochemistry	MIP	0.003-7 ng mL^{-1}	1.2 pg mL^{-1}, 266 fmol L^{-1}	Present study

Anti mAβ: Monoclonal amyloid beta antibody, SAM: Self-assembled monolayer, AuNPs: Gold nanoparticles, PrPC: Cellular prion protein, ECL: Electrochemiluminescence, mAb: Monoclonal antibody, LSPR: Localized surface plasmon resonance, ApoE4: Apolipoprotein E4, MIP: Molecularly imprinted polymer, SPR: Surface plasmon resonance, LOD: Limit of detection

PMC2813509.

3. Perani D. FDG-PET and amyloid-PET imaging: the diverging paths. *Curr Opin Neurol*. 2014;**27**(4):405-13. doi: 10.1097/WCO.0000000000000109. PubMed PMID: 24927239.
4. Zimmer ER, Leuzy A, Benedet AL, et al. Tracking neuroinflammation in Alzheimer's disease: the role of positron emission tomography imaging. *J Neuroinflammation.* 2014;**11**:120. doi: 10.1186/1742-2094-11-120. PubMed PMID: 25005532. PubMed PMCID: PMC4099095.
5. Negahdary M, Behjati-Ardakani M, Sattarahmady N, et al. Electrochemical aptasensing of human cardiac troponin I based on an array of gold nano-dumbbells-Applied to early detection of myocardial infarction. *Sensors and Actuators B: Chemical.* 2017;**252**:62-71. doi: 10.1016/j.snb.2017.05.149.
6. Rahi A, Sattarahmady N, Heli H. An ultrasensitive electrochemical genosensor for Brucella based on palladium nanoparticles. *Anal Biochem.* 2016;**510**:11-17. doi: 10.1016/j.ab.2016.07.012. PubMed PMID: 27423961.
7. Tondro GH, Vais RD, Sattarahmady N. An optical genosensor for Enterococcus faecalis using conjugated gold nanoparticles-rRNA oligonucleotide. *Sensors and Actuators B: Chemical.* 2018;**263**:36-42. doi: 10.1016/j.snb.2018.02.097.
8. Sattarahmady N, Heli H. A non-enzymatic amperometric sensor for glucose based on cobalt oxide nanoparticles. *Journal of Experimental Nanoscience*. 2012;**7**(5):529-46. doi: 10.1080/17458080.2010.539275.
9. Heli H, Majdi S, Sattarahmady N, Parsaei A. Electrocatalytic oxidation and sensitive detection of deferoxamine on nanoparticles of Fe 2 O 3@ NaCo [Fe (CN) 6]-modified paste electrode. *Journal of Solid State Electrochemistry*. 2010;**14**(9):1637-47. doi: 10.1007/s10008-010-1002-3.
10. Korecká L, Vytřas K, Bílková Z. Immunosensors in Early Cancer Diagnostics: From Individual to Multiple Biomarker Assays. *Curr Med Chem*. 2018;**25**(33):3973-87. doi: 10.2174/0929867324666171121101245. PubMed PMID: 29165064.
11. Heli H, Majdi S, Sattarahmady N. Fe2O3 core–NaCo [Fe (CN) 6] shell nanoparticles—Synthesis and characterization. *Materials Research Bulletin*. 2010;**45**(7):850-8. doi: 10.1016/J.MATERRESBULL.2010.03.006.
12. Sattarahmady N, Heli H, Vais RD. A flower-like nickel oxide nanostructure: Synthesis and application for choline sensing. Talanta. 2014;119:207-13. doi: 10.1016/j.talanta.2013.11.002. PubMed PMID: 24401406.
13. Rahi A, Karimian K, Heli H. Nanostructured materials in electroanalysis of pharmaceuticals. *Anal Biochem*. 2016;**497**:39-47. doi: 10.1016/j.ab.2015.12.018. PubMed PMID: 26751130.
14. Vais RD, Sattarahmady N, Karimian K, Heli H. Green electrodeposition of gold hierarchical dendrites of pyramidal nanoparticles and determination of azathioprine. *Sensors and Actuators B: Chemical.* 2015;**215**:113-8. doi: 10.1016/j.snb.2015.03.014.
15. Galozzi S, Marcus K, Barkovits K. Amyloid-β as a biomarker for Alzheimer's disease: quantification methods in body fluids. *Expert Rev Proteomics.* 2015;**12**(4):343-54. doi: 10.1586/14789450.2015.1065183. PubMed PMID: 26153725.
16. Song L, Lachno DR, Hanlon D, Shepro A, et al. A digital enzyme-linked immunosorbent assay for ultrasensitive measurement of amyloid-β 1–42 peptide in human plasma with utility for studies of Alzheimer's disease therapeutics. *Alzheimers Res Ther*. 2016;**8**(1):58. doi: 10.1186/s13195-016-0225-7. PubMed PMID: 27978855. PubMed PMCID: PMC5160015.
17. Sole-Domenech S, Johansson B, Schalling M, et al. Analysis of opioid and amyloid peptides using time-of-flight secondary ion mass spectrometry. *Anal Chem.* 2010;**82**(5):1964-74. doi: 10.1021/ac902712f. PubMed PMID: 20121067.
18. Sen JW, Bergen HR, Heegaard NH. On-Line Immunoaffinity-Liquid Chromatography– Mass Spectrometry for Identification of Amyloid Disease Markers in Biological Fluids. *Anal Chem*. 2003;**75**(5):1196-202. doi: 10.1021/ac026174b. PubMed PMID: 12641241.
19. Pan J, Han J, Borchers CH, Konermann L. Conformer-specific hydrogen exchange analysis of Aβ (1–42) oligomers by top-down electron capture dissociation mass spectrometry. *Anal Chem.* 2011;**83**(13):5386-93. doi: 10.1021/ac200906v. PubMed PMID: 21635007.
20. Kaneko N, Yoshimori T, Yamamoto R, et al. Multi epitope-targeting immunoprecipitation using F (ab′) fragments with high affinity and specificity for the enhanced detection of a peptide with matrix-assisted laser desorption ionization-time-of-flight mass spectrometry. *Anal Chem.* 2013;**85**(6):3152-9. doi: 10.1021/ac303344h. PubMed PMID: 23394179.
21. Watanabe KI, Ishikawa C, Kuwahara H, Sato K, et al. A new methodology for simultaneous quantification of total-Aβ, Aβx-38, Aβx-40, and Aβx-42 by column-switching LC/MS/MS. *Anal Bioanal Chem*. 2012;**402**(6):2033-42. doi: 10.1007/s00216-011-5648-1. PubMed PMID: 22200927.
22. Inoue K, Hosaka D, Mochizuki N, Akatsu H, et al. Simultaneous determination of post-translational

racemization and isomerization of N-terminal amyloid-β in Alzheimer's brain tissues by covalent chiral derivatized ultraperformance liquid chromatography tandem mass spectrometry. *Anal Chem.* 2014;**86**(1):797-804. doi: 10.1021/ac403315h. PubMed PMID: 24283798.

23. Ilkhani H, Sarparast M, Noori A, Bathaie SZ, et al. Electrochemical aptamer/antibody based sandwich immunosensor for the detection of EGFR, a cancer biomarker, using gold nanoparticles as a signaling probe. *Biosens Bioelectron.* 2015;**74**:491-7. doi: 10.1016/j.bios.2015.06.063. PubMed PMID: 26176209.
24. Kang DY, Lee JH, Oh BK, Choi JW. Ultra-sensitive immunosensor for β-amyloid (1–42) using scanning tunneling microscopy-based electrical detection. *Biosens Bioelectron.* 2009;**24**(5):1431-6. doi: 10.1016/j.bios.2008.08.018. PubMed PMID: 18829296.
25. Higuchi M, Iwata N, Matsuba Y, Sato K, et al. 19 F and 1 H MRI detection of amyloid β plaques in vivo. *Nat Neurosci.* 2005;**8**(4):527-33. doi: 10.1038/nn1422. PubMed PMID: 15768036.
26. Liu B, Shen H, Hao Y, Zhu X, et al. Lanthanide functionalized metal–organic coordination polymer: toward novel turn-on fluorescent sensing of amyloid β-peptide. *Anal Chem.* 2018;**90**(21):12449-55. doi: 10.1021/acs.analchem.8b01546. PubMed PMID: 30110150.
27. Koronyo-Hamaoui M, Koronyo Y, Ljubimov AV, Miller CA, et al. Identification of amyloid plaques in retinas from Alzheimer's patients and noninvasive in vivo optical imaging of retinal plaques in a mouse model. *Neuroimage.* 2011;**54**(Suppl 1):S204-17. doi: 10.1016/j.neuroimage.2010.06.020. PubMed PMID: 20550967. PubMed PMCID: PMC2991559.
28. Nesterov EE, Skoch J, Hyman BT, et al. In vivo optical imaging of amyloid aggregates in brain: design of fluorescent markers. *Angew Chem Int Ed Engl.* 2005;**44**(34):5452-6. doi: 10.1002/anie.200500845. PubMed PMID: 16059955.
29. Agdeppa ED, Kepe V, Liu J, Flores-Torres S, et al. Binding characteristics of radiofluorinated 6-dialkylamino-2-naphthylethylidene derivatives as positron emission tomography imaging probes for β-amyloid plaques in Alzheimer's disease. *J Neurosci.* 2001;**21**(24):RC189. doi: 10.1523/JNEUROSCI.21-24-j0004.2001. PubMed PMID: 11734604. PubMed PMCID: PMC6763047.
30. Palmqvist S, Zetterberg H, Blennow K, et al. Accuracy of brain amyloid detection in clinical practice using cerebrospinal fluid β-amyloid 42: a cross-validation study against amyloid positron emission tomography. *JAMA Neurol.* 2014;**71**(10):1282-9. doi: 10.1001/jamaneurol.2014.1358. PubMed PMID: 25155658.
31. Palladino P, Aura AM, Spoto G. Surface plasmon resonance for the label-free detection of Alzheimer's β-amyloid peptide aggregation. *Anal Bioanal Chem.* 2016;**408**(3):849-54. doi: 10.1007/s00216-015-9172-6. PubMed PMID: 26558762.
32. Huang Y, Wang R. Review on fundamentals, preparations and applications of imprinted polymers. *Current Organic Chemistry.* 2018;**22**(16):1600-18. doi: 10.2174/1385272822666180711120045.
33. Tuwahatu CA, Yeung CC, Lam YW, Roy VA. The molecularly imprinted polymer essentials: curation of anticancer, ophthalmic, and projected gene therapy drug delivery systems. *J Control Release.* 2018;**287**:24-34. doi: 10.1016/j.jconrel.2018.08.023. PubMed PMID: 30110614.
34. Pan J, Chen W, Ma Y, Pan G. Molecularly imprinted polymers as receptor mimics for selective cell recognition. *Chem Soc Rev.* 2018;**47**(15):5574-87. doi: 10.1039/c7cs00854f. PubMed PMID: 29876564.
35. Bossi A, Bonini F, Turner AP, Piletsky SA. Molecularly imprinted polymers for the recognition of proteins: the state of the art. *Biosens Bioelectron.* 2007;**22**(6):1131-7. doi: 10.1016/j.bios.2006.06.023. PubMed PMID: 16891110.
36. Ma Y, Shen XL, Wang HS, Tao J, et al. MIPs-graphene nanoplatelets-MWCNTs modified glassy carbon electrode for the determination of cardiac troponin I. *Anal Biochem.* 2017;**520**:9-15. doi: 10.1016/j.ab.2016.12.018. PubMed PMID: 28024754.
37. Silva BV, Rodríguez BA, Sales GF, et al. An ultrasensitive human cardiac troponin T graphene screen-printed electrode based on electropolymerized-molecularly imprinted conducting polymer. *Biosens Bioelectron.* 2016;**77**:978-85. doi: 10.1016/j.bios.2015.10.068. PubMed PMID: 26544873.
38. Yazdani Z, Yadegari H, Heli H. A molecularly imprinted electrochemical nanobiosensor for prostate specific antigen determination. *Anal Biochem.* 2019;**566**:116-25. doi: 10.1016/j.ab.2018.11.020. PubMed PMID: 30472220.
39. Ribeiro JA, Pereira CM, Silva AF, Sales MG. Electrochemical detection of cardiac biomarker myoglobin using polyphenol as imprinted polymer receptor. *Anal Chim Acta.* 2017;**981**:41-52. doi: 10.1016/j.aca.2017.05.017. PubMed PMID: 28693728.
40. Kaplan M, Kilic T, Guler G, Mandli J, et al. A novel method for sensitive microRNA detection: Electropolymerization based doping. *Biosens Bioelectron.* 2017;**92**:770-8. doi: 10.1016/j.bios.2016.09.050. PubMed PMID: 27836600.

41. Sharma PS, Wojnarowicz A, Sosnowska M, et al. Potentiometric chemosensor for neopterin, a cancer biomarker, using an electrochemically synthesized molecularly imprinted polymer as the recognition unit. *Biosens Bioelectron.* 2016;**77**:565-72. doi: 10.1016/j.bios.2015.10.013. PubMed PMID: 26476014.
42. Dąbrowski A. Adsorption-from theory to practice. *Adv Colloid Interface Sci.* 2001;**93**(1-3):135-224. doi: 10.1016/S0001-8686(00)00082-8. PubMed PMID: 11591108.
43. Giles HC. The history and use of the Freundlich adsorption isotherm. *Journal of the Society of Dyers and Colourists*. 1973;**89**(8):287-91. doi: 10.1111/j.1478-4408.1973.tb03158.x.
44. Zakaria ND, Yusof NA, Haron J, Abdullah AH. Synthesis and evaluation of a molecularly imprinted polymer for 2,4-Dinitrophenol. *Int J Mol Sci*. 2009;**10**(1):354-65. doi: 10.3390/ijms10010354. PubMed PMID: 19333450. PubMed PMCID: PMC2662454.
45. Kanazawa KK, Diaz AF, Geiss RH, et al. 'Organic metals': polypyrrole, a stable synthetic 'metallic'polymer. *Journal of the Chemical Society, Chemical Communications.* 1979;(19):854-5. doi: 10.1039/C39790000854.
46. Menaker A, Syritski V, Reut J, Öpik A, et al. Electrosynthesized surface-imprinted conducting polymer microrods for selective protein recognition. *Advanced Materials.* 2009;**21**(22):2271-5. doi: 10.1002/adma.200803597.
47. Bosserdt M, Erdőssy J, Lautner G, Witt J, et al. Microelectrospotting as a new method for electrosynthesis of surface-imprinted polymer microarrays for protein recognition. *Biosensors Bioelectron.* 2015;**73**:123-9. doi: 10.1016/j.bios.2015.05.049. PubMed PMID: 26056955.
48. Karimian N, Vagin M, Zavar MH, et al. An ultrasensitive molecularly-imprinted human cardiac troponin sensor. *Biosens Bioelectron.* 2013;**50**:492-8. doi: 10.1016/j.bios.2013.07.013. PubMed PMID: 23911771.
49. Moreira FT, Sharma S, Dutra RA, Noronha JP, et al. Protein-responsive polymers for point-of-care detection of cardiac biomarker. *Sensors and Actuators B: Chemical.* 2014;**196**:123-32. doi: 10.1016/j.snb.2014.01.038.
50. Dechtrirat D, Jetzschmann KJ, Stöcklein WF, Scheller FW, Gajovic-Eichelmann N. Protein rebinding to a surface-confined imprint. *Advanced Functional Materials.* 2012;**22**(24):5231-7. doi: 10.1002/adfm.201201328.
51. Tretjakov A, Syritski V, Reut J, Borozniak R, et al. Surface molecularly imprinted polydopamine films for recognition of immunoglobulin G. *Microchimica Acta.* 2013;**180**(15):1433-42. doi: 10.1007/s00604-013-1039-y.
52. Li L, Yang L, Xing Z, Lu X, Kan X. Surface molecularly imprinted polymers-based electrochemical sensor for bovine hemoglobin recognition. *Analyst.* 2013;**138**(22):6962-8. doi:10.1039/c3an01435e.
53. Li Y, Li Y, Hong M, Bin Q, Lin Z, et al. Highly sensitive protein molecularly imprinted electro-chemical sensor based on gold microdendrites electrode and prussian blue mediatedamplification. *Biosensors Bioelectron.* 2013;**42**:612-7. doi: 10.1016/j.bios.2012.10.069.
54. Jetzschmann KJ, Jágerszki G, Dechtrirat D, et al. Vectorially imprinted hybrid nanofilm for acetylcholinesterase recognition. *Advanced Functional Materials*. 2015;**25**(32):5178-83. doi: 10.1002/adfm.201501900.
55. Chen HJ, Zhang ZH, Luo LJ, Yao SZ. Surface-imprinted chitosan-coated magnetic nanoparticles modified multi-walled carbon nanotubes biosensor for detection of bovine serum albumin. *Sensors and Actuators B: Chemical.* 2012;**163**(1):76-83. doi: 10.1016/j.snb.2012.01.010.
56. Chen HJ, Zhang ZH, Xie D, Cai R, et al. Surface-Imprinting Sensor Based on Carbon Nanotubes/Graphene Composite for Determination of Bovine Serum Albumin. *Electroanalysis.* 2012;**24**(11):2109-16. doi: 10.1002/elan.201200375.
57. Cieplak M, Szwabinska K, Sosnowska M, et al. Selective electrochemical sensing of human serum albumin by semi-covalent molecular imprinting. *Biosens Bioelectron*. 2015;**74**:960-6. doi: 10.1016/j.bios.2015.07.061. PubMed PMID: 26258876.
58. Viswanathan S, Rani C, Ribeiro S, Delerue-Matos C. Molecular imprinted nanoelectrodes for ultra sensitive detection of ovarian cancer marker. *Biosens Bioelectron*. 2012;**33**(1):179-83. doi: 10.1016/j.bios.2011.12.049. PubMed PMID: 22265879.
59. Ramanaviciene A, Ramanavicius A. Molecularly imprinted polypyrrole-based synthetic receptor for direct detection of bovine leukemia virus glycoproteins. *Biosens Bioelectron.* 2004;**20**(6):1076-82. doi: 10.1016/j.bios.2004.05.014. PubMed PMID: 15556351.
60. Lien TT, Takamura Y, Tamiya E, Mun'delanji CV. Modified screen printed electrode for development of a highly sensitive label-free impedimetric immunosensor to detect amyloid beta peptides. *Anal Chim Acta*. 2015;**892**:69-76. doi: 10.1016/j.aca.2015.08.036. PubMed PMID: 26388476.
61. Kaushik A, Shah P, Vabbina PK, Jayant RD, et al. A label-free electrochemical immunosensor for beta-amyloid detection. *Analytical Methods.*

2016;**8**(31):6115-20.

62. Yu Y, Zhang L, Li C, Sun X, Tang D, Shi G. A method for evaluating the level of soluble b-Amyloid(1–40/1–42) in Alzheimer's disease based on the binding of gelsolin to b-Amyloid peptides. *Angew Chem.* 2014;**126**(47):13046-49. doi: 10.1002/ange.201405001.
63. Liu L, He Q, Zhao F, Xia N, Liu H, Li S, Liu R, Zhang H. Competitive electrochemical immunoassay for detection of β-amyloid (1–42) and total β-amyloid peptides using p-aminophenol redox cycling. *Biosens Bioelectron.* 2014;**51**:208-12. doi: 10.1016/j.bios.2013.07.047. PubMed PMID: 23962708.
64. Zhu L, Zhang J, Wang F, Wang Y, et al. Selective amyloid β oligomer assay based on abasic site-containing molecular beacon and enzyme-free amplification. *Biosens Bioelectron*. 2016;**78**:206-212. doi: 10.1016/j.bios.2015.11.048. PubMed PMID: 26613510.
65. Rushworth JV, Ahmed A, Griffiths HH, et al. A label-free electrical impedimetric biosensor for the specific detection of Alzheimer's amyloid-beta oligomers. *Biosens Bioelectron*. 2014;**56**:83-90. doi: 10.1016/j.bios.2013.12.036. PubMed PMID: 24480125.
66. Kim CB, Choi YY, Song WK, Song KB. Antibody-based magnetic nanoparticle immunoassay for quantification of Alzheimer's disease pathogenic factor. *J Biomed Opt.* 2014;**19**(5):051205. doi: 10.1117/1.JBO.19.5.051205. PubMed PMID: 24297060.
67. Xing Y, Xia N. Biosensors for the determination of amyloid-beta peptides and their aggregates with application to Alzheimer's disease. *Analytical Letters.* 2015;**48**(6):879-93. doi: 10.1080/00032719.2014.968925.
68. Wu CC, Ku BC, Ko CH, Chiu CC, et al. Electrochemical impedance spectroscopy analysis of A-beta (1-42) peptide using a nanostructured biochip. *Electrochimica Acta.* 2014;**134**:249-57. doi: 10.1016/j.electacta.2014.04.132.
69. Kruse N, Schlossmacher MG, Schulz-Schaeffer WJ, Vanmechelen E, Vanderstichele H, El-Agnaf OM, Mollenhauer B. A first tetraplex assay for the simultaneous quantification of total α-synuclein, tau, β-amyloid42 and dj-1 in human cerebrospinal fluid. *PLoS One.* 2016;**11**(4):e0153564. doi: 10.1371/journal.pone.0153564. PubMed PMID: 27116005. PubMed PMCID: PMC4846093.
70. Liu L, Zhao F, Ma F, Zhang L, Yang S, Xia N. Electrochemical detection of β-amyloid peptides on electrode covered with N-terminus-specific antibody based on electrocatalytic O2 reduction by Aβ (1–16)-heme-modified gold nanoparticles. *Biosens Bioelectron.* 2013;**49**:231-5. doi: 10.1016/j.bios.2013.05.028. PubMed PMID: 23770394.
71. Haes AJ, Chang L, Klein WL, Van Duyne RP. Detection of a biomarker for Alzheimer's disease from synthetic and clinical samples using a nanoscale optical biosensor. *J Am Chem Soc.* 2005;**127**(7):2264-71. doi: 10.1021/ja044087q. PubMed PMID: 15713105.
72. Kang MK, Lee J, Nguyen AH, Sim SJ. Label-free detection of ApoE4-mediated β-amyloid aggregation on single nanoparticle uncovering Alzheimer's disease. *Biosens Bioelectron*. 2015;**72**:197-204. doi: 10.1016/j.bios.2015.05.017. PubMed PMID: 25982728.
73. Zhou Y, Zhang H, Liu L, Li C, et al. Fabrication of an antibody-aptamer sandwich assay for electrochemical evaluation of levels of β-amyloid oligomers. *Sci Rep*. 2016;**6**:35186. doi: 10.1038/srep35186. PubMed PMID: 27725775. PubMed PMCID: PMC5057102.
74. Carneiro P, Loureiro J, Delerue-Matos C, Morais S, Do Carmo Pereira M. Alzheimer's disease: Development of a sensitive label-free electrochemical immunosensor for detection of amyloid beta peptide. *Sensors and Actuators B: Chemical*. 2017;**239**:157-65. doi: 10.1016/j.snb.2016.07.181.
75. Rama EC, González-García MB, Costa-Garcia A. Competitive electrochemical immunosensor for amyloid-beta 1-42 detection based on gold nanostructurated Screen-Printed Carbon Electrodes. *Sensors and Actuators B: Chemical.* 2014;**201**:567-71. doi: 10.1016/j.snb.2014.05.044.
76. Veloso AJ, Chow AM, Ganesh HV, Li N, et al. Electrochemical immunosensors for effective evaluation of amyloid-beta modulators on oligomeric and fibrillar aggregation processes. *Analytical Chemistry*. 2014;**86**(10):4901-9. doi: 10.1021/ac500424t.
77. Georganopoulou DG, Chang L, Nam JM, et al. Nanoparticle-based detection in cerebral spinal fluid of a soluble pathogenic biomarker for Alzheimer's disease. *Proc Natl Acad Sci U S A.* 2005;**102**(7):2273-6. doi: 10.1073/pnas.0409336102. PubMed PMID: 15695586. PubMed PMCID: PMC548981.
78. Gagni P, Sola L, Cretich M, Chiari M. Development of a high-sensitivity immunoassay for amyloid-beta 1–42 using a silicon microarray platform. *Biosens Bioelectron.* 2013;**47**:490-5. doi: 10.1016/j.bios.2013.03.077. PubMed PMID: 23624018.
79. Li H, Cao Y, Wu X, Ye Z, Li G. Peptide-based electrochemical biosensor for amyloid β 1–42 soluble oligomer assay. *Talanta.* 2012;**93**:358-63. doi: 10.1016/j.talanta.2012.02.055. PubMed PMID: 22483923.